The coordinated replication of Vibrio cholerae 's two chromosomes required the acquisition of a unique domain by the RctB initiator

Florian Fournes, Theophile Niault, Jakub Czarnecki, Alvise Tissier-Visconti, Didier Mazel, Marie-Eve Val

Published online 13 October 2021

Nucleic Acids Research, 2021, Vol. 49, No. 19 **11119–11133**
https://doi.org/10.1093/nar/gkab903

The coordinated replication of *Vibrio cholerae*'s two chromosomes required the acquisition of a unique domain by the RctB initiator

Florian Fournes[1,2,†], Theophile Niault[1,2,3,†], Jakub Czarnecki[1,2,4], Alvise Tissier-Visconti[1,2], Didier Mazel[1,2,*] and Marie-Eve Val[1,2,*]

[1]Institut Pasteur, Université de Paris, Unité Plasticité du Génome Bactérien, Département Génomes et Génétique, Paris 75015, France, [2]Centre National de la Recherche Scientifique, UMR3525, Paris 75015, France, [3]Sorbonne Université, Collège Doctoral, Paris 75005, France and [4]University of Warsaw, Department of Bacterial Genetics, Institute of Microbiology, Faculty of Biology, Warsaw 02-096, Poland

Received April 21, 2021; Revised August 30, 2021; Editorial Decision September 16, 2021; Accepted September 22, 2021

ABSTRACT

***Vibrio cholerae*, the pathogenic bacterium that causes cholera, has two chromosomes (Chr1, Chr2) that replicate in a well-orchestrated sequence. Chr2 initiation is triggered only after the replication of the *crtS* site on Chr1. The initiator of Chr2 replication, RctB, displays activities corresponding with its different binding sites: initiator at the iteron sites, repressor at the 39m sites, and trigger at the *crtS* site. The mechanism by which RctB relays the signal to initiate Chr2 replication from *crtS* is not well-understood. In this study, we provide new insights into how Chr2 replication initiation is regulated by *crtS* via RctB. We show that *crtS* (on Chr1) acts as an anti-inhibitory site by preventing 39m sites (on Chr2) from repressing initiation. The competition between these two sites for RctB binding is explained by the fact that RctB interacts with *crtS* and 39m via the same DNA-binding surface. We further show that the extreme C-terminal tail of RctB, essential for RctB self-interaction, is crucial for the control exerted by *crtS*. This subregion of RctB is conserved in all Vibrio, but absent in other Rep-like initiators. Hence, the coordinated replication of both chromosomes likely results from the acquisition of this unique domain by RctB.**

INTRODUCTION

Genome architecture is defined in most bacterial lineages, conserved through speciation, and therefore is a fundamental question of microbial evolution. 5–10% of bacteria have a multipartite organization of their genome with at least one secondary chromosome containing essential core genes (1). Secondary chromosomes originate from plasmids that have been domesticated as *bona fide* components of the genome, as evidenced by several of their plasmid features (2). Although plasmids confer adaptive functions, which augment fitness under certain conditions, they are also frequently poorly adapted to a new genetic background and can be quickly lost in the absence of selective pressure. Therefore, their domestication as secondary chromosomes requires co-evolutionary processes involving their adaptation to host cellular mechanisms as well as accommodation of the host (3). In this study, we made an in-depth structure-function study of RctB, the replication initiator of *Vibrio cholerae* secondary chromosome, to understand the mechanism underlying the orchestrated replication of both chromosomes, which is controlled by this protein.

Like all *Vibrionaceae*, *V. cholerae* has its genome split on two circular replicons, Chr1, a main 3 Mbp-chromosome and Chr2, a secondary 1 Mbp-chromosome. The Chr1 replication origin (*ori1*) is similar to the single chromosome origin of *Escherichia coli* (*oriC*) and the ubiquitous bacterial replication initiator DnaA governs Chr1 initiation (4–6). The initiation of Chr2 replication, however, is different from that of a typical bacterial chromosome and its origin (*ori2*) is closely related to that of iteron-containing plasmids (6). Like iteron-plasmid origins, *ori2* replication initiation requires an accurate arrangement of DNA motifs comprising iterons, an IHF binding site, an AT-rich DNA unwinding element and a DnaA-box (7) (Figure 1A). Iterons are directly repeated sequences recognized by a plasmid-encoded initiator (Rep) (8). The binding of Rep to iterons near the AT-rich element promotes local DNA unwinding where replication starts (8). The specific equivalent of Rep for Vibrio

*To whom correspondence should be addressed. Tel: +33 186467361; Email: marie-eve.kennedy-val@pasteur.fr
Correspondence may also be addressed to Didier Mazel. Email: didier.mazel@pasteur.fr
†The authors wish it to be known that, in their opinion, the first two authors should be regarded as Joint First Authors.

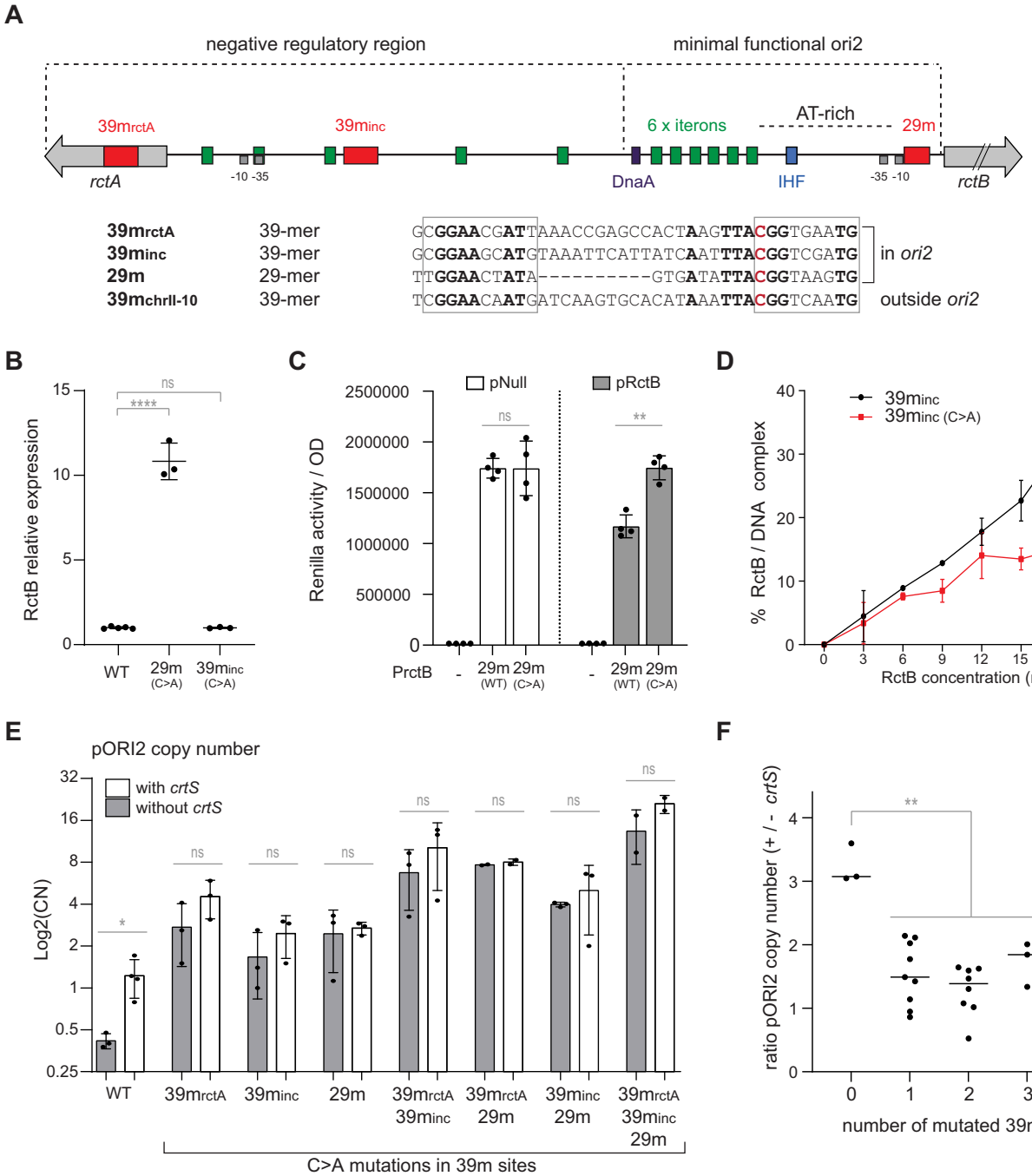

Figure 1. *crtS* counteracts 39m inhibitory activity. (**A**) Representation of Chr2 origin of replication (*ori2*) and sequence alignment of all 39m sites. RctB binding sites are indicated in green (iterons) and red (39m). All 39m contain two GC-rich repeats at both ends with an intervening 19-bp (or 9-bp) non-conserved AT-rich sequence. The imperfect GC-rich repeats are RctB binding sites (gray box), which are phased to be on the same side of the DNA helix (13). Deletion of 10 bp in the 29m intervening sequence (deletion of a full helix turn) maintains the phasing between the RctB binding sites and does not abrogate the function of the site. Conserved bases are shown in bold. The (C > A) mutation is indicated in red (18). (**B**) Expression of *rctB* relative to the housekeeping gene *gyrA* in the N16961 wild-type strain (WT), the 29m (C > A) and the $39m_{inc}$ (C > A) *V. cholerae* mutants. (**C**) Measure of repression by RctB of its promoter with and without the (C > A) mutation: 29m(WT), 29m(C > A). Promoter activity is assessed by measuring Renilla luciferase activity (Experimental set-up in Supplementary Figure S1). RctB expression is induced with 0.2% arabinose from a low-copy plasmid (pTVC11, Supplementary Table S2). The same empty plasmid is used as a control of absence of repression (pNull). Data are normalized to the optical density of each culture (OD at λ 600 nm). (**D**) Quantification of complex formation between a 40 bp DNA probe carrying a $39m_{inc}$ (with or without a C > A mutation) and increasing concentrations of RctB (nM : nanomolar), without $DnaK/J_{Vc}$ (Supplementary Figure S2). Percent of bound DNA is equal to (intensity of the shifted band/combined intensities of shifted and unbound DNA bands) x 100. (**E**) pORI2 copy number (CN) relative to the chromosome [Log_2(pORI2/*oriC*)] in *E. coli* strains with and without a chromosomal *crtS* site. pORI2 contains either 1, 2 or 3 mutated 39m sites (C > A). (**F**) Graph representing the effect of *crtS* (pORI2 *E. coli* / pORI2 *E. coli*::*crtS*) as a function of the number of mutated 39m sites (experimental values of (E)). In all graphs, data represent averages from at least three independent biological replicates ± standard deviations. Each dot represents an independent experiment. Statistics were applied on pairwise comparisons using Student's t-test and on multiple comparisons using one-way ANOVA. Statistical significances are indicated (ns : non significant; * $P < 0.05$; ** $P < 0.01$; *** $P < 0.001$; **** $P < 0.0001$).

Chr2 is called RctB (6). Similar to Rep, RctB proteins form homo-dimers in solution with a head-to-head configuration (9). As Rep, RctB dimers are monomerized by DnaJ and DnaK chaperones, which favours their binding to DNA in a cooperative manner (10–12). Iteron-type plasmids limit their copy number via a mechanism called origin-pairing or handcuffing. In this process, the coupling of origins via iteron-bound Rep protein causes steric hindrance to initiation (8). The handcuffing of *ori2* is also one of the main regulatory mechanisms that limit Chr2 copy number; however, it requires the participation of additional regulatory sequences other than iterons, which are discussed below (13).

Despite many features common to both Chr2 and iteron plasmids, the regulation of Chr2 replication involves additional functions that are not found in plasmids and which lead to a more elaborate control of Chr2 replication (13). First, Chr2 replication initiation is tightly regulated to occur only once per cell cycle, while plasmids generally initiate replication several times over the bacterial cell cycle (14,15). Secondly, Chr2 replication is initiated at a specific time of the cell cycle so that Chr1 and Chr2 complete their replication at the same time, an evolutionary selected characteristic in Vibrio (16–18). It thus seems that during their domestication, plasmid-type machineries, which are suitable for maintaining high-copy-number plasmids, have evolved towards systems capable of sustaining the replication of low-copy-number replicons in harmony with the host cell cycle (1,14). Indeed, the structure of RctB is more complex than those of Rep. RctB is a large protein (658 amino acids (AA)), twice as large as the Rep initiators (e.g. π is 305 AA, TrfA is 382 AA). RctB harbors four domains (I, II, III, IV) with three DNA binding surfaces (in domains I, II and III) (9) whereas most Rep initiators contain only two domains (N-terminal and C-terminal) with two DNA binding surfaces that bind to the two halves of the iterons (9). RctB central domains (domains II and III) are structurally related to Rep N-terminal and C-terminal domains and are essential for Chr2 replication. RctB additional domains (domains I and IV) are unique and may have emerged during the evolution of *Vibrionaceae* to help meet the stricter regulatory requirements necessary for proper chromosome maintenance (9). Domain I is essential for binding to iterons and for replication (9). Domain IV, which is not essential for replication, is however critical for limiting the number of Chr2 copies (11).

Unlike Rep, RctB specifically recognizes DNA motifs other than iterons. RctB binds to three classes of DNA sites of different sequences and sizes: the iterons (11-mer or 12-mer), the 39m sites (29-mer, 39-mer) and the *crtS* site (62-bp) (10,18) (Figure 1A). Eleven iterons are present in *ori2*, six of which are essential for replication, while the others have a regulatory function (6). Four 39m (three in *ori2* and one located 40 kb away from *ori2*) act as strong negative regulators of *ori2* initiation (13,19,20) (Figure 1A). The unique *crtS* site located on Chr1 exerts a positive regulation of Chr2 replication (20). At these three types of sites, RctB monomers specifically bind cooperatively and then oligomerize non-specifically on adjacent DNA (10). The initial binding of RctB as a monomer requires domains I, II and III (10,11). However, various DNA binding surfaces are required for binding to iterons and 39m suggesting that the binding conformation of RctB is different to these sites (9). Both the cooperative binding and oligomerization activities of RctB require its domain IV (10,11). As mentioned above, Chr2 copy number is limited by a handcuffing mechanism which is conveyed by the 39m sites that are contiguous to the iterons in *ori2* (13). In this process, iteron-bound RctB and 39m-bound RctB form a bridge that hinders the initiation of replication (11,13,21). This negative regulation of *ori2* initiation mediated by the 39m requires RctB domain IV. A large deletion of RctB domain IV (Δ157) causes loss of handcuffing activity and a copy-up phenotype (11). More specifically, a 71 AA region in domain III-IV (AA 450 to 521) has been extensively characterized and found to be involved in Chr2 copy number limitation, DNA binding and RctB dimerization (22).

The above-mentioned knowledge of Chr2 replication regulation mechanisms is insufficient to explain how the initiation of Chr2 replication is synchronized with Chr1 replication. This coordination requires the third RctB binding site, *crtS* (18), located in trans, halfway between the origin and the terminus of Chr1 (20). Upon replication, *crtS* triggers the initiation of Chr2, therefore its location on Chr1 ensures termination synchrony of the two chromosomes (18). The deletion of *crtS* severely impairs growth and is associated with the loss of Chr2 (18). It was proposed that *crtS* could act as a DNA chaperone to remodel RctB to an active form with altered DNA binding activities to iteron and 39m sites (20,23). In this study, we dissected RctB to better understand how *crtS* steers Chr2 replication. We found that *crtS* triggers Chr2 initiation by acting as an anti-inhibitory site, preventing the 39m sites from negatively regulating replication. This *crtS* activity involves the same RctB DNA binding region that is required for the binding to the 39m. The action of *crtS* also involves a protein-protein interaction domain located at the extreme carboxy-terminal end of RctB. We propose that the cooperative binding of RctB to DNA, mediated by protein-protein interactions, is necessary for *crtS* activity as an anti-inhibitor of the 39m.

MATERIALS AND METHODS

Bacterial strains, plasmids and nucleotides

All *E. coli* and *V. cholerae* strains and plasmids used in this study are listed in Supplementary Tables S1 and S2. Further details regarding their engineering are provided in the Supplementary Methods. The oligonucleotide sequences used for dPCR, RT-dPCR, *in vitro* experiments and cloning purposes are listed in Supplementary Table S3.

Protein purification

The expression plasmids derived from pET32b were transformed into *E. coli* BL21-DE3 (Supplementary Table S2). Plasmids used to express the RctB HTH mutants were built as described in (9). Proteins were produced and purified as described in (10). More details are provided in Supplementary Methods.

In vitro experiments

Electrophoretic Mobility Shift Assays (EMSA) of double-stranded DNA probes containing the RctB *crtS*, 39m or

iteron binding sites were radiolabeled in 5'-end [γ32P]. A 114-bp long probe containing *crtS* was generated by PCR as described in (10). The iteron-containing probes were methylated *in vitro* as described in (10). The resulting labeled probes were used in a binding reaction performed as described in (10) and analyzed with the Typhoon FLA 9500 laser scanner. All protein concentrations are indicated in the figure legends. More details are provided in Supplementary Methods.

Bacterial Two-hybrid

BTH101 cells were co-transformed with plasmids encoding a T18 N-fusion of RctB and a T25 N-fusion of RctB according to the instructions described in (24). The different plasmid combinations are described in Tables S2. Co-transformants were selected on LB agar plates containing carbenicillin (100 μg/ml) and kanamycin (25 μg/ml). Co-transformants were pooled, resuspended in 100 μl of LB medium, and spotted (5 μl drop of cell suspension) onto LB agar plates containing X-Gal (40 μg/ml), IPTG (0.5 mM), carbenicillin (100 μg/ml), and kanamycin (25 μg/ml). Plates were incubated for 2 days at 30°C, followed by an additional 24 h at 4°C. Blue spots indicate protein–protein interactions.

Digital PCR quantification of DNA loci (dPCR)

Quantifications of (*ori1* and *ori2*) in *V. cholerae* and (*oriC* and pORI2) in *E. coli* were performed as described in (10) using multiplex digital PCR (Stilla Technologies) (25). Primers and probes are listed in Supplementary Table S3. Total genomic DNA was purified using the DNeasy Blood & Tissue Kit (QIAGEN). PCR reactions were performed with 0.1 ng of DNA using the PerfeCTa® MultiPlex qPCR ToughMix® (Quantabio) on a Sapphire chip (Stilla Technologies). Digital PCR was conducted on a Naica Geode and Image acquisition on the Naica Prism3 reader. Images were analyzed Crystal Miner software (Stilla Technologies). The dPCR run was performed using the following steps : droplet partition (40°C, atmospheric pressure AP to + 950mbar, 12 min), initial denaturation (95°C, +950 mbar, for 2 min), followed by 45 cycles at (95°C for 10 s and 60°C for 30 s), droplet release (down 25°C, down to AP, 33 min). More details are provided in Supplementary Methods.

Digital PCR quantification of RNA (RT-dPCR)

Quantification of RctB mRNA was performed in *V. cholerae* from exponentially growing cultures (OD_{600} 0.4) using multiplex digital RT-dPCR (Stilla Technologies) (25). Primers and probes are listed in Supplementary Table S3. *V. cholerae* RNA was prepared as described in (26). PCR reactions were performed with 1 ng of RNA using the qScript™ XLT One-Step RT-qPCR ToughMix® (Quantabio). RT-dPCR and data analysis were conducted as described above for dPCR. The RT-dPCR run was performed in the following steps: droplet partition (40°C, AP to +950 mbar, 12 min), cDNA synthesis (50°C, +950 mbar, 10 min), initial denaturation (95°C, +950 mbar, for 1 min), followed by 45 cycles at (95°C for 10 s and 60°C for 15 s), droplet release (down 25°C, down to AP, 33 min). Expression values were normalized to the expression of the housekeeping gene *gyrA* as described in (26). More details are provided in Supplementary Methods.

Luciferase assay

E. coli reporter strains were engineered with a *lacZ* insertion containing the *renilla* luciferase gene (27) under the control of PrctA or PrctB promoters. More details for generating reporter strains are provided in the Supplementary Methods. Reporter strains were transformed with the plasmid pTVC11 containing a transcriptional fusion of *rctB-firefly* luciferase genes under the P_{BAD} promoter (28). Overnight cultures from transformed cells were diluted 1:100 in Mueller-Hinton medium supplemented with 50 μg/ml spectinomycin and 0.2% arabinose and grown to an OD_{600} ∼0.5. To 50μl of reporter cell culture, we added 40 μl of *E. coli* cell culture (J665, OD_{600} 0.5) and 10 μl of a KH_2HPO_4 (1M)–EDTA (20 mM) solution. The mixture was placed on dry ice for 5 min and left to equilibrate at room temperature for 15 min. The cells were then lysed with 300 μl of a lysis buffer for 10 min. Both luciferase activities of Firefly and Renilla were sequentially measured using the dual-luciferase reporter assay (DLR, Promega) following the manufacturer's recommendations. 20 μl of the lysed extract was added to 100 μl of Firefly substrate (LARII) in a glass tube. The light emission was acquired for 10 s in a luminometer (Lumat LB9507, Berthold). Quenching of Firefly luciferase luminescence and concomitant activation of Renilla luciferase was achieved by adding 100 μl of STOP&GLO Reagent to the tube. Light emission from Renilla activity was acquired for 10 s. Luminescence data were normalized to the OD_{600}. MG1655 wild-type cultures were used as non-luminescent controls.

RESULTS

crtS exerts a positive control on Chr2 replication by counteracting the inhibitory activity of 39m

We previously isolated mutations in *ori2* that compensate for the loss of *crtS* in *V. cholerae* (18). In particular, we identified a mutation in the 29-mer site (29m) located in the promoter region of the *rctB* gene. This mutation is an adenine substitution of a cytosine (C > A), which is conserved at all 39m sites (Figure 1A), indicating the importance of this nucleotide. In addition to its role in hindering *ori2* initiation via handcuffing, the binding of RctB to the 29m represses its own transcription (19). We tested the impact of the C > A mutation on RctB expression in *V. cholerae* by RT-dPCR. We observed that RctB is 10 times more expressed when the 29m sequence contains the C > A mutation than in the WT strain or in a mutant where the C > A mutation is inserted in a 39m site outside the RctB promoter region ($39m_{inc}$) (Figure 1B). Overexpression of RctB could thus be due to a lack of self-repression due to a decrease in RctB binding to the 29m in its promoter region. Since RctB binding to the 29m represses the activity of its own promoter (19), we used this repression as a

proxy to monitor RctB binding *in vivo*. We developed a luciferase reporter tool in *E. coli* by fusing the promoter region of RctB (PrctB) to a Renilla luciferase reporter gene. RctB fused to a Firefly luciferase gene is supplied on a low-copy plasmid (PrctB) under the control of an arabinose-inducible promoter (P_{BAD}) (Supplementary Figure S1A). Using a dual-luciferase assay system, we can both monitor RctB binding to 39m by measuring PrctB activity (via Renilla-generated luminescence measurement) while controlling the induction of RctB expression on the plasmid (via Firefly-generated luminescence measurement). As expected, upon RctB induction (Supplementary Figure S1B, pink bars), PrctB activity decreased significantly (Supplementary Figure S1B, blue bars). In absence of RctB (Figure 1C, pNull), the C > A mutation in the 29m site in the promoter region of RctB (PrctB-$29m_{(C>A)}$) had no impact on Renilla expression compared to the WT promoter (PrctB-$29m_{(WT)}$) meaning that the C > A mutation in the 29m does not interfere with the activity of the promoter. In presence of RctB (Figure 1C, pRctB), the level of expression of Renilla decreased significantly in PrctB-$29m_{(WT)}$ but remained unchanged with PrctB-$29m_{(C>A)}$. Therefore, the C > A mutation alters the repressive activity of RctB by altering its binding to the 29m. We further assessed whether the impact of the C > A mutation on RctB binding was also detrimental at other 39m sites. We chose to test the effect of this mutation on the $39m_{inc}$ site, because RctB binds to this site similarly as to the 29m site (19). *In vitro*, we observed a decrease in RctB/DNA complex formation when the $39m_{inc}$ site is mutated, which corroborates our *in vivo* observation on the 29m (Figure 1D, Supplementary Figure S2). EMSA showed that both DNA probes containing either wild-type or mutated 39m sites mainly formed C2 complexes with RctB (i.e. the 39m is bound by two molecules of RctB, (10)), suggesting that the C > A mutation does not affect the cooperative binding of RctB to 39m (Supplementary Figure S2). We further studied the impact of mutating all three 39m sites in *ori2* on the control of replication by *crtS*. We used an artificial replication system in *E. coli*, using a plasmid, pORI2, which replication depends solely on *ori2* (10). By quantitative digital PCR (dPCR), we monitored pORI2 copy number (CN) variation in *E. coli* MG1655 without and with a *crtS* chromosomal site. In *E. coli*, the presence of *crtS* upregulates pORI2 copy number (10). We then introduced the C > A mutations at the three 39m sites of the pORI2, either individually, in pairs or all three together, and measured the relative copy number of pORI2 in the absence or presence of *crtS*. As expected, since the 39m are strong inhibitory sites, their incremental mutations resulted in an increase in the copy number of pORI2 in absence of *crtS* (Figure 1E – without *crtS*, Supplementary Figure S3A). Furthermore, we revealed that *crtS* no longer has any effect on the control of pORI2 copy number when the 39m sites carry the C > A mutation, regardless of which site has been mutated (Figure 1E – with *crtS*, Supplementary Figure S3B). Surprisingly, the control by *crtS* was lost once a single site was mutated (Figure 1F). Since each of the C > A mutations renders the 39m sequence insensitive to *crtS* activity, it is likely that *crtS* inhibits the handcuffing activity of the 39m and not only the transcriptional control role of RctB through its binding to the 29m. All these results strongly suggest that *crtS* upregulates the initiation of replication at *ori2*, primarily by neutralizing the inhibitory effect of 39m.

The binding of RctB to *crtS* and 39m involves the same DNA binding surface

To understand how *crtS* competes with the 39m sites, we investigated which RctB DNA binding surfaces are involved in its interaction with *crtS*. RctB harbours three winged-helix-turn-helix motifs (HTH1, HTH2, HTH3) in domains I, II and III respectively, that mediate binding to DNA (9). As no full length RctB structure is currently available, we used a recently released AlphaFold2-MMseqs2 webserver to generate a model of RctB complete structure (29,30) which we visualized with ChimeraX (31) (Figure 2A, Video S1). This predicted structure shows that the three HTH motifs are close together in a pocket that could accommodate a DNA molecule. This structure is in agreement with Orlova's model (9) which speculates that domain I and domain II–III bind opposite faces of the iteron DNA site. They showed that all three HTH are crucial for RctB binding to iterons, but only HTH2 is essential for the binding to 39m (9). To explore the importance of these HTHs in *crtS* binding, we purified the three RctB HTH mutants ($RctB_{HTH1}$, $RctB_{HTH2}$, $RctB_{HTH3}$) and confirmed that their affinities for 39m were as described in (9) (Supplementary Table S2, Supplementary Figure S4). We further compared the binding of $RctB_{HTH1}$, $RctB_{HTH2}$, $RctB_{HTH3}$ to the binding of $RctB_{WT}$ by EMSA with a radiolabelled DNA probe containing the *crtS* site (Figure 2B). With all four RctBs tested (WT and HTH mutants), we observe the formation of higher molecular weight complexes. This observation depends on the ability of several RctB monomers to bind cooperatively to DNA (10). Thus, all three $RctB_{HTH}$ mutants retain their ability to bind cooperatively to DNA. Quantification of the formation of RctB-*crtS* complexes at increasing RctB concentrations reveals that RctB, $RctB_{HTH1}$ and $RctB_{HTH3}$ have the same affinity for *crtS* while $RctB_{HTH2}$ hardly forms complex with *crtS* (Figure 2C). At the highest concentration of the $RctB_{HTH2}$ mutant, we could observe the formation of a higher molecular weight nucleoprotein complex, meaning that $RctB_{HTH2}$ is still able to bind cooperatively to *crtS* (10). Thus, the disruption of HTH2 strongly reduced the binding efficiency of RctB to the *crtS* site as it is the case for the 39m without abolishing its ability to bind cooperatively. This suggests that the binding conformation of RctB, involving domain II, could be similar for 39m and *crtS*. Consistent with these results, the addition of non-radioactive *crtS* DNA competitor reduces the formation of RctB/39m complexes *in vitro* while the interactions between iterons and RctB are not altered by the addition of *crtS* (Supplementary Figure S5). Since 39m and *crtS* compete for RctB binding, we wondered if *crtS* could partially be substituted by a 39m in *V. cholerae* on Chr1. To do so, we first inserted the three types of RctB binding sites (iteron, 39m and *crtS*) into the Tn7 insertion site (*attTn7*) located on the Chr1 of *V. cholerae*, and then excised the native *crtS* site (Δ*crtS*). Using digital PCR (dPCR), we measured the copy number variation between Chr1 and Chr2 of non-replicating *V. cholerae* bearing either of the RctB sites on Chr1 (Figure 2D). If the RctB binding site is fully

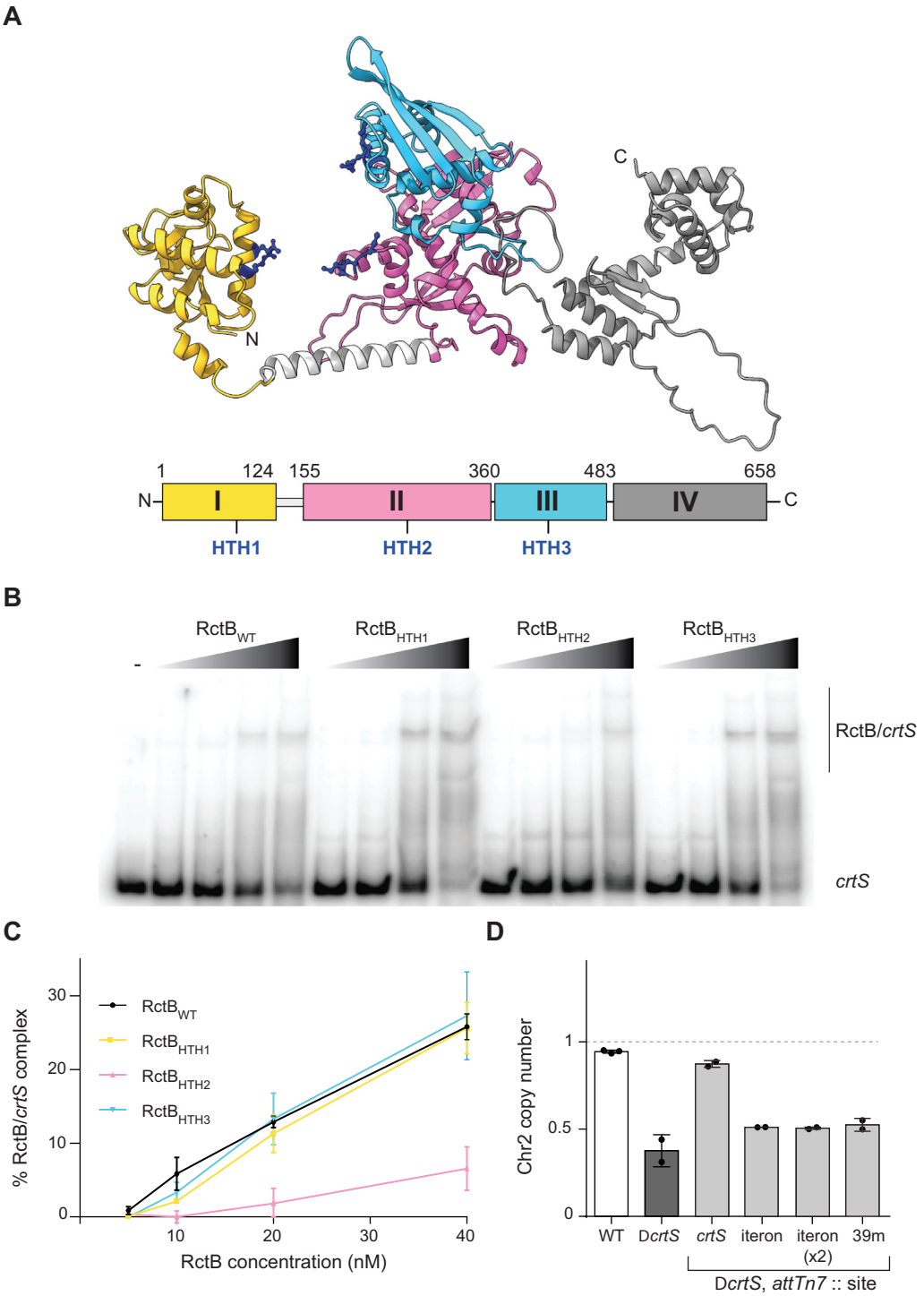

Figure 2. RctB share the same DNA binding surface to bind to *crtS* and 39m. (**A**) Model of RctB structure predicted with AlphaFold2 (29) and visualized with ChimeraX (31). The four domains of RctB, described by Orlova (9), are shown with the same color code in the secondary structure model and in the linear representation of RctB below. The three winged-helix-turn-helix motifs in domains I, II and III are indicated HTH1, HTH2 and HTH3 on the linear representation of RctB. The AAs that we mutated into these HTH motifs are shown in dark blue on the secondary structure model. (**B**) Electrophoretic mobility shift assays of wild-type RctB ($RctB_{WT}$) and HTH mutants: $RctB_{HTH1}$ (Q83A-R84A-R86A), $RctB_{HTH2}$ (K271A-K272A-S274A) and $RctB_{HTH3}$ (R420A-R423A) with a 114bp-probe containing a *crtS* site. RctB concentration for each gel is incremented as follows: 5, 10, 20, 40 nM. (**C**) Mean percentage of RctB/DNA complex formation with *crtS* in three EMSA experiments (± standard deviation). Percent of bound DNA is calculated as in Figure 1D. (**D**) Chr2 copy number relative to Chr1 (*ori2*/*ori1*) in non-replicating *V. cholerae*. In all mutants, the native *crtS* site is deleted and RctB binding sites are inserted in the *attTn7* insertion site of Chr1 (mean ± standard deviation).

active in triggering Chr2 replication, we expect a Chr2 copy number (*ori2*/*ori1* ratio) of about 1 (e.g. WT). If the site is inactive, Chr2 will be lost which will translate into a lower Chr2 copy number (e.g. Δ*crtS*, *attTn7*::Ø). Our results show that only *crtS* can trigger Chr2 replication when located on Chr1 and cannot be substituted by any other RctB binding site (i.e. 39m, 1 or 2 iterons). Although the binding of RctB to *crtS* and 39m appears to be similar, only *crtS* can perform its function, suggesting that the triggering of Chr2 initiation by *crtS* may involve other activities of RctB.

RctB domain IV is necessary for both 39m and *crtS* regulation of *ori2* initiation

Although RctB domain IV is not essential for replication initiation, its role in Chr2 copy number control is fundamental (11). Domain IV encompasses RctB handcuffing activity and RctB oligomerization ability, both of which are mediated by protein-protein interactions (10,11,22). We investigated whether these activities could be involved in *crtS*-mediated control of Chr2 replication. To circumvent the toxic effect of Chr2 over-replication in *V. cholerae* caused by the deletion of RctB domain IV, we used our reporter plasmid pORI2 in *E. coli* (10). We built a set of pORI2 with truncations from RctB domain IV by inserting stop codons in the *rctB* gene (Figure 3A). All the truncated versions of pORI2 could replicate autonomously except for the complete deletion of domain IV (ΔIV) for which the few clones that we obtained integrated pORI2 into the chromosome. We measured the copy number of all pORI2 truncated RctB mutants by quantitative dPCR (Figure 3B). We observed that most of the truncations in domain IV increase pORI2 copy number. Only the deletion of 2 AA in RctB (Δ2) had no impact on pORI2 copy number compared to WT (Figure 3B, white bars). We noticed that, depending on the size of the truncation, there were two levels of increase in pORI2 copy number, suggesting that the negative control of *ori2* replication occurs at two levels in RctB domain IV. Larger deletions of domain IV (Δ157, Δ147, Δ137) considerably increased pORI2 copy number by a factor of about 50 (Figure 3B, dark grey bars). We found that these large deletions overlap with a 71 AA regulatory region previously identified for its role in limiting *ori2* initiation, DNA binding and RctB/RctB interactions (22). Shorter deletions (Δ101, Δ82, Δ41, Δ27, Δ17) moderately increased pORI2 copy number by a factor of about 4 (Figure 3B, light grey bars). This region closer to the carboxyl-terminal end of RctB has not yet been studied nor identified for its role in controlling Chr2 replication. To assess the role of RctB domain IV in *crtS*-mediated control of replication, we perform the same assay in *E. coli* carrying a *crtS* site inserted in the chromosome (Figure 3C, Supplementary Figure S6). We observed that most of the deletions in domain IV abolished the control of *crtS* on pORI2 copy number (Figure 3C, +/− *crtS* ∼1). Only the shortest deletion of RctB (Δ2) did not abolish the control of *crtS* over pORI2 copy number (Figure 3C, +/− *crtS* > 3). We further assessed the *in vivo* binding of a selection of truncated variants (ΔIV, Δ147, Δ82, Δ17, Δ2) to the 39m sites by measuring the activity of the Renilla reporter transcribed from the RctB promoter (including a 29m) as in Figure 1C. We observed that in the presence of RctB, Renilla's activity increased significantly in all truncated mutants (ΔIV, Δ147, Δ82, Δ17) with the exception of RctBΔ2, to a level equivalent to that obtained in the absence of RctB (Figure 3D). This result means that mutants (ΔIV, Δ147, Δ82, Δ17) are no longer able to repress the 39m-containing RctB promoter. In parallel, we assessed the *in vivo* binding of RctB to iteron sites by measuring the activity of the Renilla reporter transcribed from the *rctA* promoter (PrctA contains two iterons and no 39m sites) as described in (11). Unlike PrctB, the *rctA* promoter remains repressed by all RctB mutants (ΔIV, Δ147, Δ82, Δ17, Δ2) as well as by RctB WT (Supplementary Figure S7), which suggests that domain IV mutations have no impact on the regulation of iteron-containing PrctA. Thus Chr2 replication regulation by 39m and *crtS* entails the domain IV of RctB. These results reinforce the hypothesis that the binding of RctB to 39m is crucial in the control of Chr2 replication by *crtS*.

The extreme C-terminal of RctB domain IV is crucial for replication coordination by *crtS*

Unlike the other RctB domains, the entire domain IV or its segments have not been crystallized. Our AlphaFold2 structure prediction shows that domain IV is poorly structured between AA 480 and 538 and that the C-terminal part contains a well-structured module (Figure 2A, Video S1). More precisely, the secondary structure prediction analysis of RctB revealed a region with high probability to form an α-helix within the last 16 AA C-terminal extremity (Figure 4A and Supplementary Figure S8). To assess its role in Chr2 replication control and *crtS* activity, we performed an alanine scanning in the 16 AA C-terminal tail of RctB. Substitutions with alanines are expected to alter the interactions in the α-helix without causing major disruption of the overall protein folding (32). We substituted, three residues at a time, 15 AA with alanines (Figure 4A, left panel). The pORI2 mutants were then analysed by quantitative dPCR to measure the effect of alanine substitutions on their copy number and on *crtS* activity. All pORI2 mutants have a copy number that is not significantly affected compared to the WT (Supplementary Figure S9), meaning that the negative regulatory control is still functional when the α-helix is mutated. However, whether mutations were inside or outside the α-helix, the influence of *crtS* on pORI2 copy number is different (Figure 4A, right panel). When RctB is mutated upstream or downstream of the α-helix, the +/− *crtS* ratio is higher than 1 meaning the *crtS* still exerts a role on pORI2 replication control. When RctB is mutated in the α-helix, the +/− *crtS* ratio is close 1, which means that *crtS* no longer influences pORI2 replication. We further substituted a conserved leucine located in the middle of the α-helix with a proline (L651P) in order to disrupt the α-helix (32). With the $RctB_{L651P}$ mutation, *crtS* has no longer an effect on pORI2 copy number, whereas with a substitution outside the α-helix, RctBG657P, *crtS* increases pORI2 copy number to a level similar to wild-type (Figure 4A). Thanks to the mild copy-up phenotype caused by the $RctB_{L651P}$ mutation (Supplementary Figure S9), we were able to insert this mutation into *V. cholerae* without it being lethal which allowed us study its effect under endogenous conditions. We

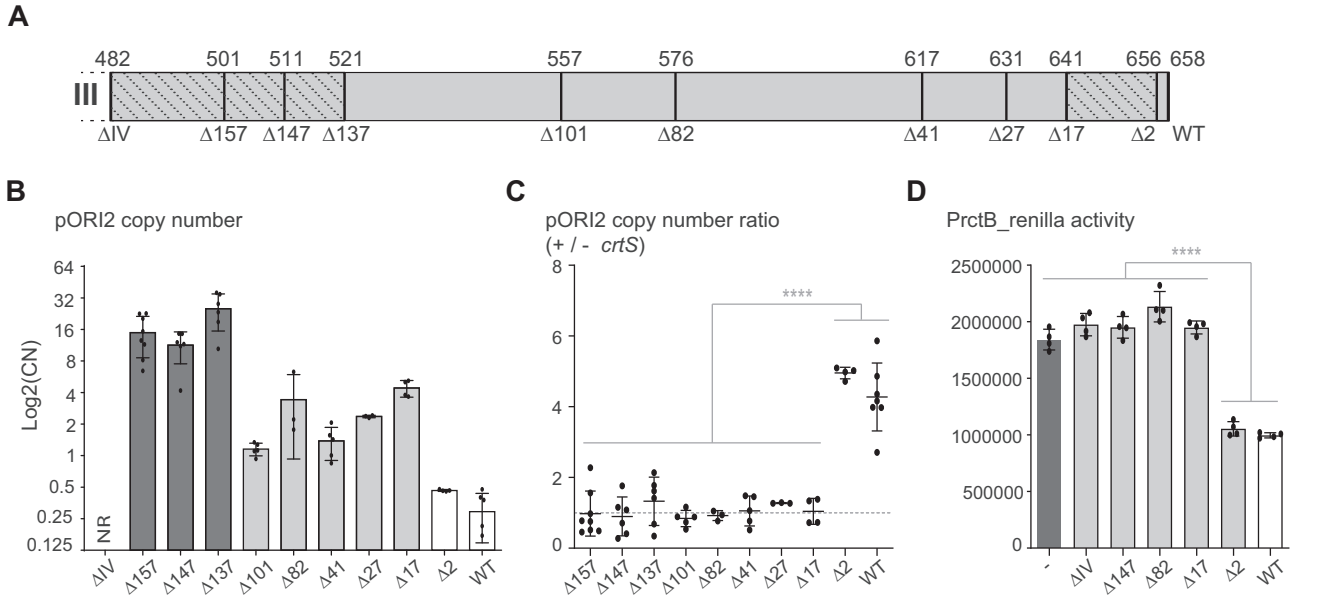

Figure 3. *crtS* regulation of Chr2 replication involves RctB domain IV. (**A**) Domain IV representation of RctB. Stop codons were inserted to generate truncated proteins as indicated in amino acids coordinates (above, AA) and amino acids deletion (bottom, ΔAA). (**B**) Copy-number (CN) of pORI2 relative to the chromosome in *E. coli* strains. The various pORI2 derivatives were built by inserting stop codons in *rctB* as indicated in panel A. The Y-axis represents [Log2(CN)]. NR means not replicative. The different shades of grey represent the two different levels of up-regulation of *ori2* replication upon truncation of domain IV (dark grey: very high 32 > CN > 8; light grey : moderately high 4 > CN > 1). (**C**) Ratio of pORI2 copy number in *E. coli* with and without a chromosomal *crtS* site (+/− *crtS*). An absence of activation by *crtS* corresponds to a ratio of 1 (indicated by a dashed line). (**D**) Promoter repression by RctB (and truncated mutants) binding to the 29m in PrctB, as Figure 1C. RctB and mutants are induced with arabinose (0.2%) from a low-copy plasmid (Supplementary Table S2). In all graphs, data represent averages from at least three independent biological replicates ± standard deviations. Each dot represents an independent experiment. Statistics were applied on pairwise comparisons using Student's *t*-test and on multiple comparisons using one-way ANOVA. Statistical significances are indicated (ns : non significant; * $P < 0.05$; ** $P < 0.01$; *** $P < 0.001$; **** $P < 0.0001$).

measured the *ori2*/*ori1* ratios in presence or absence of the native *crtS* site both in non-replicating (stationary phase) and replicating (exponential phase) conditions to differentiate the effect of *crtS* on Chr2 copy number and Chr2 initiation timing respectively (Figure 4B). We observed that the $RctB_{L651P}$ mutation causes a doubling of the Chr2 copy number compared to Chr1. As in *E. coli*, Chr2 copy number in the $RctB_{L651P}$ mutant of *V. cholerae* is no longer under the influence of *crtS*, whereas it maintains a Chr1:Chr2 ratio of 1:1 in the WT strain (Figure 4B, stationary phase, *ori2*/*ori1* = 1 in WT with native *crtS*). We also observed, in exponential phase, that the timing of Chr2 replication in the $RctB_{L651P}$ mutant is no longer controlled by *crtS* (Figure 4B, exponential phase, *ori2*/*ori1* < 1 in WT with native *crtS*). In the $RctB_{L651P}$ mutant, *crtS* thus no longer has control over the copy number and the timing of initiation of Chr2. We further characterized $RctB_{L651P}$ for its promoter repressing activity on PrctB (containing a 29m) and PrctA (containing two iterons) using the luciferase reporter. On PrctB, the Renilla activity, using $RctB_{L651P}$, is similar to results obtained with the empty plasmid (Figure 4C) while on PrctA, it is similar to results obtained with $RctB_{WT}$. This observation means that $RctB_{L651P}$ is still capable of repressing PrctA but not PrctB. This de-repression of PrctB was confirmed in *V. cholerae* by RT-dPCR in a $RctB_{L651P}$ mutant where the expression level of RctB increases to >20-fold that of WT (Supplementary Figure S10A). We compared the amount of RctB protein by Western blot in both the 29m(C > A) and $RctB_{L651P}$ *V. cholerae* mutants where Chr2 replication initiation is no longer under the control of *crtS* (Supplementary Figure S10B). In the 29m(C > A) mutant, we saw an increase in the amount of RctB protein. However, in the $RctB_{L651P}$ mutant, the amount of RctB protein was unaltered compared to WT. This suggests that increasing the amount of RctB is not the only way to overcome the control by *crtS*. The defective binding of $RctB_{L651P}$ to 39m sites could cause the independence of Chr2 replication from *crtS* control. The predicted α-helix in the C-terminal tail of RctB is conserved among 26 Vibrio species with the leucine at position 651 being fully conserved (Supplementary Figure S11). We tested the effect of mutating this leucine in two phylogenetically distant *Vibrio* species (*Vibrio nigripulchritudo* and *Grimontia hollisae*). We generated pORI2 derivatives containing the [*ori2*-rctB] regions of *V. nigripulchritudo* and *G. hollisae* that we introduced into *E. coli* containing a chromosomal copy of their corresponding *crtS* sites. Both *V. nigripulchritudo* and *G. hollisae* pORI2 copy number increases in the presence of their respective *crtS* sites in *E. coli*, as it does for *V. cholerae* pORI2 (Figure 4D). When the last leucine of RctB is mutated (*V. cholerae* $RctB_{L651P}$, *V. nigripulchritudo* $RctB_{L651P}$ and *G. hollisae* $RctB_{L653P}$), the copy number of the respective pORI2 is no longer controlled by *crtS* (Figure 4D). Note that in *G. hollisae*, the L653P mutation is not copy-up as it is for *V. cholerae* and *V. nigripulchritudo*. These results show that the unique C-terminal tail of RctB is critical in the control of Chr2 replication by *crtS* and that it is conserved among *Vibrionaceae*.

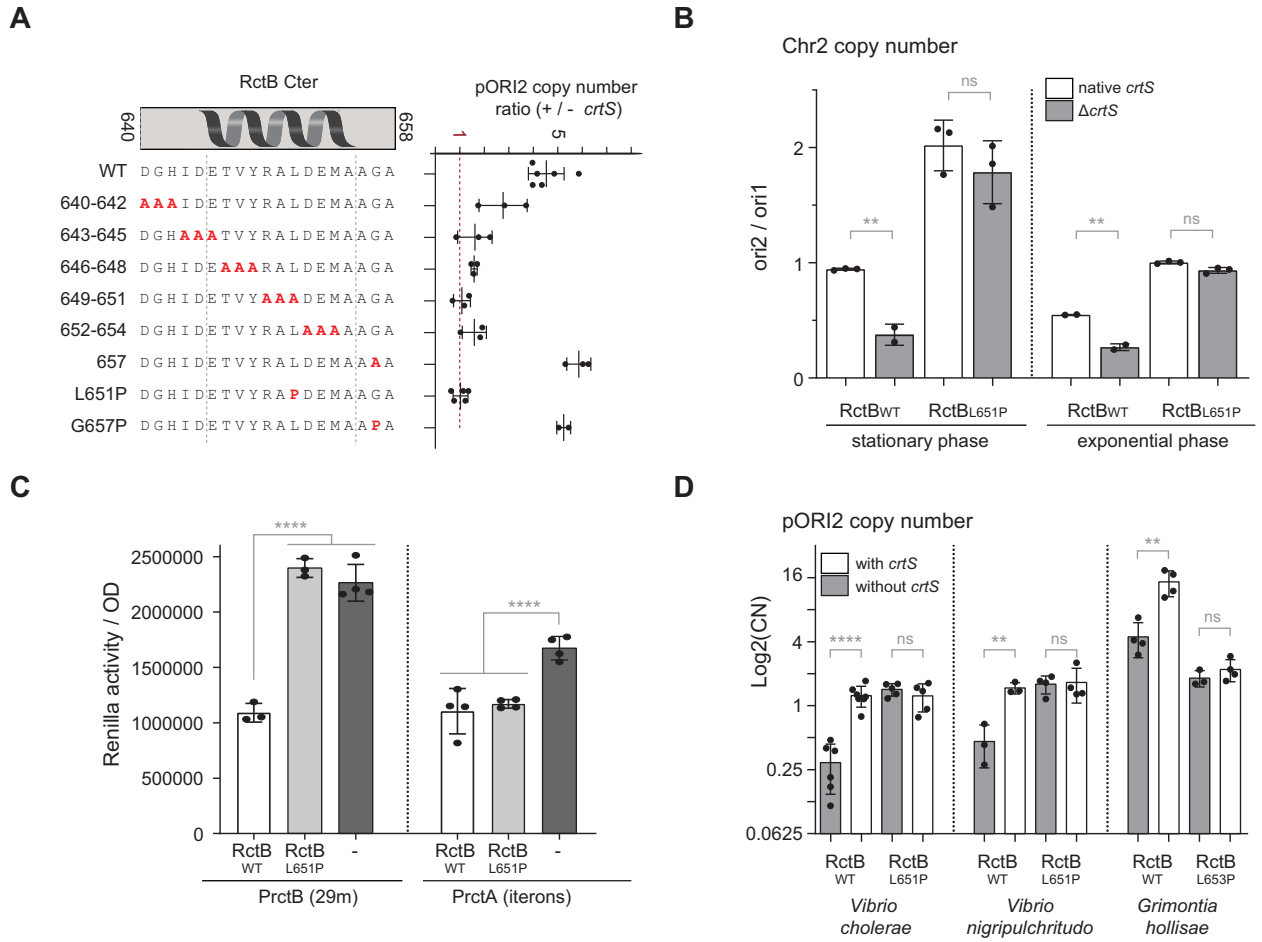

Figure 4. The C-terminal tail of RctB is essential for the control of Chr2 replication by *crtS*. (**A**) Mutagenesis of the last 19 AA in the carboxy-terminal end of RctB. Left panel: The coordinates of the putative alpha helix (645 to 655 AA), based on Supplementary Figure S8D, are indicated by a dashed line. Alanine and proline substitutions are indicated below the wild-type sequence (WT) in red. Right panel: Ratio of pORI2 copy number in *E. coli* with and without a chromosomal *crtS* site (+/− *crtS*) (data from Supplementary Figure S9). An absence of activation by *crtS* corresponds to a ratio of about 1 (indicated by the red dashed line). (**B**) *ori2* copy number relative to *ori1* (*ori2*/*ori1*) in *V. cholerae* wild-type ($RctB_{WT}$) or with a point mutation in RctB ($RctB_{L651P}$) in presence (native *crtS*) or absence (Δ*crtS*) of *crtS*. Total genomic DNA was purified either from replicating cells (exponential phase) or from non-replicating cells (stationary phase). (**C**) Promoter repression by $RctB_{WT}$ and $RctB_{L651P}$ mutants of PrctB (29m) or PrctA (iterons) as in Figure 1C. RctB is induced with arabinose (0.2%) from a low-copy plasmid (Supplementary Table S2). (**D**) Copy number of pORI2 derivatives relative to the *E. coli* chromosome (pORI2/*oriC*). The pORI2 derivatives carrying the *ori2* and *rctB* genes from either *V. cholerae*, *V. nigripulchritudo* or *G. hollisae* are transformed into *E. coli* strains carrying their respective *crtS* sites. In all graphs, data represent averages from at least three independent biological replicates ± standard deviations. Each dot represents an independent experiment. Statistics were applied on pairwise comparisons using Student's *t*-test and on multiple comparisons using one-way ANOVA. Statistical significances are indicated (ns : non significant; * $P < 0.05$; ** $P < 0.01$; *** $P < 0.001$; **** $P < 0.0001$).

The extreme C-terminal of domain IV supports RctB self-interaction

In an earlier study, we showed that the domain IV of RctB is required for the cooperative binding and further non-specific oligomerization of RctB onto DNA after its initial specific binding (10). RctBΔIV is no longer able to oligomerize on iterons even in the presence of DnaK/J chaperones which stimulate RctB cooperative binding (10). For this reason, we explored the *in vitro* binding activities of the RctB truncated mutants on all three binding sites. None of the mutants with deletions ranging from AA 101 to 17, as well as the $RctB_{L651P}$ mutant, could be produced in soluble form. We were however able to purify RctBΔ157, RctBΔ147 and RctBΔ2. We compared their binding activities to $RctB_{WT}$ and RctBΔIV by EMSA using probes carrying either a 39-mer, a methylated iteron or a *crtS* site in the presence or absence of DnaK/J chaperones (Supplementary Figure S12). RctBΔIV, RctBΔ157 and RctBΔ147 could hardly form the complex C3 on a 39m site (i.e. three RctB molecules bound to the probe, (10)), even in presence of DnaK/J, suggesting an alteration of RctB oligomerization activity (Figure 5A, Supplementary Figure S12A). Conversely, RctBΔ2 could still form C3 complexes similar to $RctB_{WT}$. Similar results were observed with probes containing *crtS* (Supplementary Figure S12B) and methylated iterons (Supplementary Figure S12C). RctBΔIV, RctBΔ157 and RctBΔ147 formed mainly C1 complexes with iterons and *crtS*, whereas RctBΔ2 bound similarly to $RctB_{WT}$ to all the DNA probes. We quantified the formation of C3 complexes, reflecting the

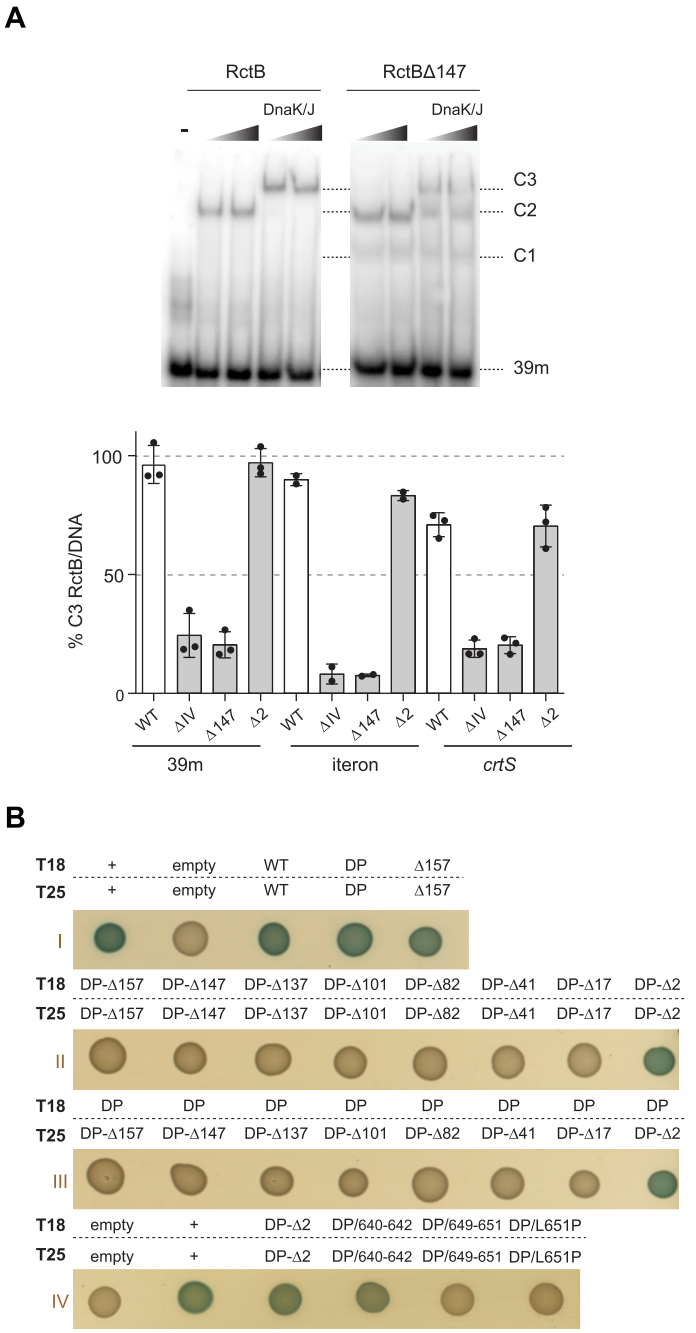

Figure 5. RctB domain IV is involved in RctB self-interaction and cooperative DNA binding. (**A**) Top panel : Example of cooperative binding of RctB and RctBΔ147 to 39m by EMSA. Free DNA probes (39m) and RctB nucleoprotein complexes (C1, C2 and C3 = 1, 2 and 3 bound RctB respectively) are indicated (as in (10)). The protein concentrations are 10 nM or 20 nM RctB with constant concentrations of 5 nM $DnaK_{Vc}$ and 5 nM $DnaJ_{Vc}$. Bottom panel: percentage of RctB/DNA higher complex formation (C3) in EMSA shown in Supplementary Figure S12. EMSAs were performed with RctB (WT) or domain IV mutants (IV, Δ147, Δ2) with DNA probes containing either a 39m site, an iteron, or a *crtS* site. Quantifications were done under conditions using 10 nM RctB and in the presence of $DnaK/J_{Vc}$ chaperones. Percent of C3 RctB/DNA complexes is equal to (intensity of the C3 shifted band/combined intensities of C1, C2, C3 shifted bands) × 100. Mean of at least two independent experiments ± standard deviation. Each dot represents one replicate. (**B**) Bacterial two-hybrid interactions of RctB with itself in *E. coli* on X-Gal plates. Blue indicates interaction and white indicates no interaction. Panel (I) shows the positive leucine zipper (+/+) and negative (empty/empty) controls of interaction, the interactions of $RctB_{WT}$ with itself (WT/WT) and the interactions of the two single mutants $RctB_{D314P}$ (DP/DP) and deletion of 157 AA in domain IV (Δ157/Δ157) with themselves. Panels (II) and (III) show the interactions that were tested with RctB double mutants having an increasing deletion of domain IV (DP/ΔAA). Panel (II): interaction of the double mutants with themselves. Panel (III): interaction of the double mutants with the single mutant $RctB_{D314P}$ (DP). Panel (IV) shows the interactions that were tested within the last C-terminal predicted α-helix of RctB. The vectors used for bacterial two-hybrid are described in Supplementary Table S2.

oligomerization activity of RctB, and observed that the mutant RctBΔ147, like the mutant RctBΔIV, is defective for oligomerization (Figure 5A, Bottom panel). Because we failed to purify mutants from the C-terminal region of domain IV (between amino acids AA 557 and 656), including the $RctB_{L651P}$ mutant, we were unable to characterize them *in vitro*. To circumvent this issue, since RctB oligomerization on DNA depends on protein-protein interactions involving its domain IV (10), we used the bacterial two-hybrid system in *E. coli* to test RctB/RctB interactions *in vivo* in all RctB truncated mutants (24). First, in order to observe only the interactions mediated by domain IV and because other RctB-RctB interactions are mediated in the dimerization interface of domain II (9), we inserted a D314P (DP) mutation that kills this interaction. As expected, with only one mutation (DP or Δ157), RctB interactions still occur, as shown by blue spots (Figure 5B, panel I). With both mutations (DP and Δ157), RctB no longer interact, as shown by white spots (Figure 5B, panel II). Among all the truncated mutants of domain IV, only RctBΔ2 displays a blue spot suggesting that residues between 641 (RctBΔ17) and 656 (RctBΔ2) are involved in RctB/RctB interactions (Figure 5B, panel II). These interactions take place symmetrically between the extreme C-terminal 16 AA region of each RctB partner since the impairment of only one partner is sufficient to disrupt the interaction (Figure 5B, panel III). We confirmed that none of the domain IV mutations interfered with RctB expression or overall folding using single mutants (no mutation of D314) (Supplementary Figure S13). We further tested the role of the last C-terminal 16 AA in RctB/RctB interactions. We observed that RctB mutants in the predicted α-helix no longer interact with each other (Figure 5B, panel IV, DP/649–651 and DP/L651P) while mutants outside the α-helix still interact (Figure 5B, panel IV, DP/640–642). These results show that the C-terminal extreme tail of RctB is necessary for its self-interaction. Thus, the coordination of Chr1 and Chr2 replication most likely relies on the ability of RctB molecules to interact via their C-terminal extremities, presumably in order to bind cooperatively onto DNA.

DISCUSSION

Replication in *V. cholerae* is a very sophisticated process that ensures synchronous replication of both chromosomes once per cell cycle (17). The initiation of Chr2 replication is subordinated to Chr1 replication via the *crtS* locus (18). The initiator of Chr2 replication, RctB, has structural similarities with the initiators of Rep-type plasmids via its core domains, II and III (9). However, these plasmids are generally not replicated in synchrony with their host cell cycle. Besides, RctB is more complex than Rep-type initiators as it carries two additional domains providing new functions (9). Understanding how RctB relays the information between *crtS* and *ori2* to initiate Chr2 replication is critical to our comprehension of the mechanisms that maintain both chromosomes in harmony with the cell cycle. From our observations, we propose that *crtS* triggers the initiation of Chr2 replication by acting as an anti-inhibitory site, preventing 39m from negatively regulating replication. This activity relies on a unique sub-structure, found in the extreme C-terminal tail of RctB, conserved in all Vibrio, but absent from the other Rep-type initiators. Deletion or disorganization of this element, lead to lose the Chr2 replication control by *crtS*, as well as of the orchestrated replication of *V. cholerae*'s two chromosomes. Therefore, the coordinated replication of the two chromosomes of Vibrio likely results from the acquisition of this unique functional domain by RctB.

crtS acts as an anti-inhibitor of the 39m sites

Chr2 origin contains three negative regulatory 29/39m sites, which exert a tight control on Chr2 copy number (Figure 1A). We previously identified that a single nucleotide mutation (C > A) in the 29m site of the RctB promoter was able to compensate the deleterious effect of *crtS* deletion in *V. cholerae* by increasing Chr2 copy number (18). We show here that the (C > A) mutation alters RctB binding to 29m and 39m, both *in vivo* (Figure 1C) and *in vitro* (Figure 1D). In the 29m, the C > A mutation causes a 10-fold increase in RctB expression in *V. cholerae* (Figure 1B), which we thought could explain the rescue of the *crtS* mutant by the increased amount of initiator (18). However, the same mutation in a 39m outside the RctB promoter also increases pORI2 copy number and compensates *crtS* deletion, while it has no effect on RctB expression (Figure 1B, E). Therefore, the (C > A) mutation must alter another mechanism implicated in 39m negative regulation of *ori2* replication. By weakening the RctB affinity for the 39m, the C > A mutation could hamper *ori2* handcuffing and reduce competition for RctB binding to the iterons. In *E. coli*, the (C > A) mutation in one, two, or all three 39m sites increases the copy number of pORI2 with a cumulative effect (Supplementary Figure S3) indicating that all 39m sites are involved in *ori2* negative regulation. However, the (C > A) mutation in either of the 39m sites makes pORI2 replication independent of *crtS* (Figure 1E, F). This indicates that in *E. coli,* the control of *crtS* on *ori2* replication requires the fully functional set of 39m sites. We could not verify this in *V. cholerae* as we were not able to mutate more than one 39m site at a time nor could we mutate the 39m site in *rctA*. It is possible that our failure to generate 39m mutants in *V. cholerae* is due to the lethality induced by these mutations since they lead to an increase in Chr2 copy number which is known to be toxic for the bacterium (33).

Baek *et al*. observed in *E. coli*, that the presence of *crtS* decreased the binding of RctB to 39m (20). Our *in vitro* observations are in agreement with these results, as we showed that linear *crtS* competes with linear 39m for binding to RctB (Supplementary Figure S5). Moreover, we show that RctB binds to *crtS* via its domain II DNA-binding surface (Figure 2B, C). Since the same DNA-binding surface of RctB is required for binding to a 39m (Supplementary Figure S4) (9), competition between the two sites seems structurally evident. Baek *et al*. also observed in *E. coli*, that the presence of *crtS* increased the binding of RctB to iterons (20). In our experiments, we observed that linear *crtS* DNA does not compete with methylated iterons (Supplementary Figure S5). This observation means that the *crtS* effect on RctB-iterons interaction is not reproducible in our *in vitro* condition. We use $DnaK_{Vc}$ and $DnaJ_{Vc}$ from *V. cholerae*,

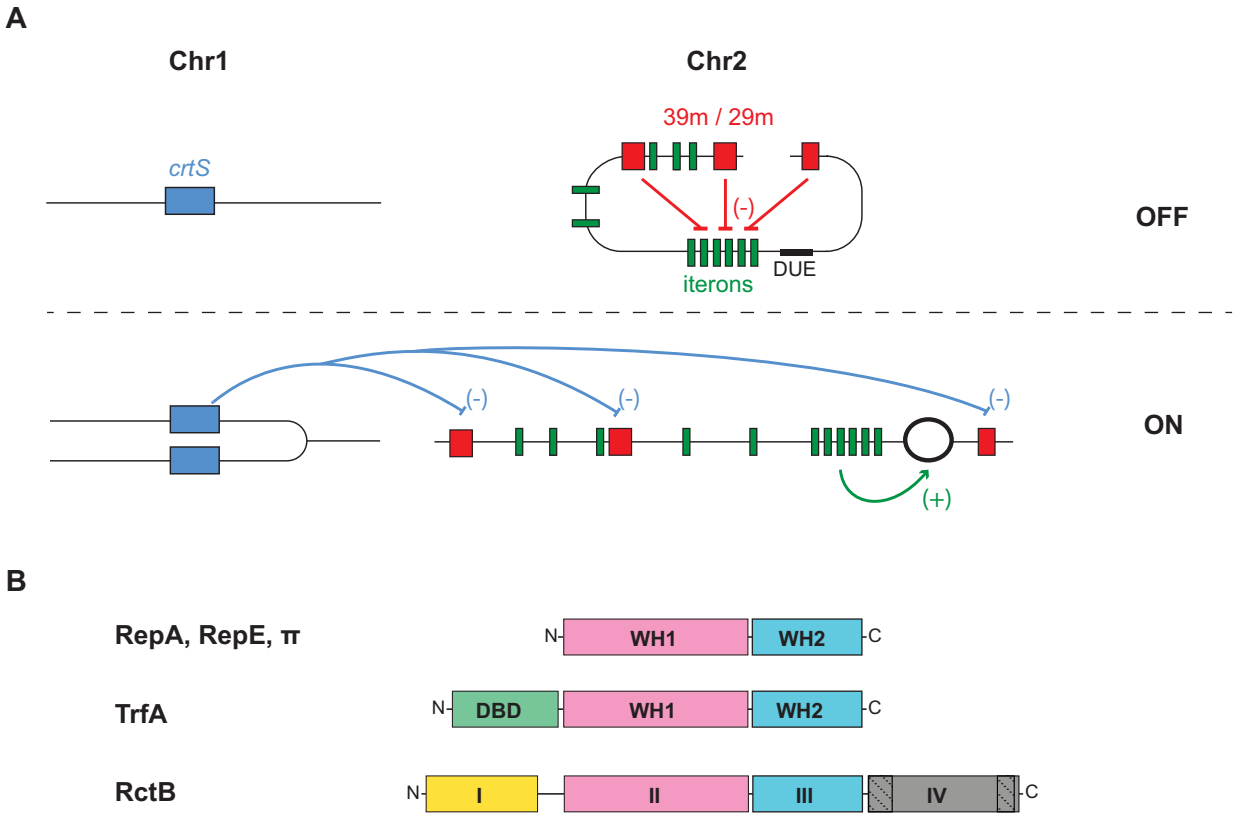

Figure 6. Model for coordination of replication between Chr1 and Chr2 by *crtS*. (**A**) RctB binding sites are shown in green (iterons), red (39m) and blue (*crtS*). A positive control is represented by an arrow associated with (+), and a negative control is represented by a flat-ended arrow associated with (−). **OFF** = Chr1: *crtS* has not been replicated. Chr2: RctB binding to the 39m sites inhibits replication initiation at *ori2* mainly by handcuffing (red arrows). **ON** = Chr1: *crtS* has been replicated. We hypothesize that the transient binding of RctB to the replicated *crtS* sites results in either a competition with the 39m sites or a remodeling of RctB that results in a decrease in its affinity for the 39m sites (blue arrows). Chr2: RctB binding to 39m is inhibited which releases *ori2*. Binding of RctB to methylated iterons causes opening of the DNA unwinding element (DUE) and oligomerization of RctB onto single-stranded DNA (green arrows) (7). (**B**) Acquisition of a unique domain IV by the initiator RctB to coordinate replication of Chr1 and Chr2. Comparison of protein domain organization of three types of iteron initiators. The different structural domains are indicated (WH = winged helix, DBD = DNA binding Domain). Additional N-ter domains (such as the domain I of RctB) have been found in TrfA-like plasmid initiators (DBD) (43). The role of domain I in RctB is still elusive. Additional C-terminal domains (such as the domain IV of RctB) have not found in iteron-like plasmid initiators. RctB domain IV is crucial for coordinating Chr1 and Chr2 replication. Representation adapted from (43).

whereas previous studies have been performed with $DnaK_{Ec}$ and $DnaJ_{Ec}$ from *E. coli* (20). We already observed such discrepancies in the binding of RctB to its DNA substrates between *E. coli* and *V. cholerae* (10). This suggests that species-specific interactions between $DnaK_{Vc}/J_{Vc}$ and RctB are important to promote the binding of additional RctB monomers to DNA (10).

In conclusion, it appears that the positive control of *crtS* on *ori2* replication initiation occurs through the abolishment of 39m inhibitory activities. Competition for RctB binding between *crtS* and 39m could impede the handcuffing of *ori2* by 39m, allowing replication to be initiated. Importantly, a 39m does not functionally replace *crtS*, even in trans on *V. cholerae* Chr1 (Figure 2D), implying that RctB–*crtS* and RctB–39m interactions are different; only the RctB–*crtS* interaction can exert a role in initiating Chr2 replication. How the interactions between RctB–*crtS* and RctB–39m differ is not yet understood, and may be due either to the specific DNA sequences contained in *crtS* or to the binding of the transcription factor Lrp (34).'

The self-interaction of RctB molecules through their C-terminal tails is crucial for *crtS* control of Chr2 replication

The down-regulation of *ori2* replication initiation by RctB requires its domain IV (11). This domain, whose structure is still unknown, does not harbor a known DNA binding motif, although it has been shown to bind to DNA (9,22). However, domain IV is required for RctB handcuffing and oligomerization activities (10,11,22). We used the recently released AlphaFold2 algorithm (29), which uses machine learning to predict protein structures with high accuracy, in order to predict the full length RctB secondary structure (Figure 2A, Video S1). This gives us new information about how RctB may interact with DNA and with itself. In this model, it clearly seems that all three HTH are close together within a pocket that could accommodate the DNA molecule, in agreement with Orlova's model (9). We also see that RctB domain IV is separated from the other three domains. It is therefore conceivable that RctB C-terminal part is more accessible to interact with the C-terminal module of another RctB molecule. This would be consistent with our

in vivo observations of domain IV-domain IV interactions (Figure 5B).

In this study, we discovered a novel function of domain IV, which allows for the positive regulation of Chr2 replication by *crtS*. All domain IV RctB truncated mutants, except for RctBΔ2, are no longer regulated by *crtS* (Figures 3C, 4A, B). This is in contrast to published results showing replication-stimulating activity by *crtS* in the RctBΔ157 mutant (20). These discrepancies can be explained by our different setups. In our system, *crtS* is inserted into the *E. coli* chromosome and the entire [*ori2*-RctB] region is on the same plasmid, whereas in Baek's setup three plasmids contain the three components separately: RctB, *ori2* and *crtS*. In our study, once the integrity of domain IV is affected, the replication-enhancing activity of *crtS* is lost in *E. coli* (Figures 3C, 4A) and this observation was confirmed in *V. cholerae* (Figure 4B).

We observed that RctB domain IV includes at least two regions of replication regulation, which are reflected by two levels of Chr2 copy limitation (Figure 3B). The first region, between AA 501 and 521 (Figure 3A), overlaps a regulatory region previously characterized for its role in Chr2 copy number down-regulation, binding to DNA and RctB dimerization (22). In both plasmids and Chr2, handcuffing is the main safeguard mechanism that keeps copy number low. Increasing the concentration of initiator above the physiological level does not significantly increase plasmid copy number, whereas altering handcuffing can drastically increase plasmid copy number (8). Since all three RctBΔ157, RctBΔ147 and RctBΔ137 mutants are deleted for the dimerization interface involved in handcuffing, this explains the high pORI2 copy number (Figure 3B). *In vivo*, RctB handcuffing mutants can be studied in *E. coli* using pORI2 (Figure 3B) but not in *V. cholerae* because these mutations are likely to be lethal due to the toxicity caused by excessive Chr2 copy number. These RctB domain IV mutants (RctBΔ157, RctBΔ147 and RctBΔ137) are defective in cooperatively binding to DNA (Figure 5A, Supplementary Figure S12). These mutants preferentially form C1 complexes with DNA, corresponding to the binding of a monomer of RctB to DNA (10). This implies that the cooperative binding of RctB is not required for initiation of *ori2* replication. Plasmid initiators catalyze origin opening via a DNA distortion mechanism (35,36). DNA distortion is induced by binding of the plasmid initiator to an iteron array (37,38). It is likely that binding of RctB to the six-iteron array of *ori2* catalyzes the initiation of *ori2* replication by mediating a change in DNA conformation (7) without requiring RctB cooperative binding to DNA.

The second, newly identified region between AA 641 and 656 (Figure 3A, Supplementary Figure S9) is mildly involved in the control of Chr2 copy number (Figure 3B). All truncations from Δ17 to Δ101 have the same mild impact on pORI2 copy number. Between Δ2 and Δ17 truncations resides a predicted α-helix, conserved in other *Vibrionaceae* (Supplementary Figures S8, S11). We show that this putative α-helix is crucial for *crtS* control of *ori2* replication (Figure 4A) whereas its disruption has only a limited impact on pORI2 copy number (Supplementary Figure S9) indicating that the α-helix is not involved in the negative control of RctB via handcuffing with 39m. When a leucine of the alpha helix is substituted with a proline (L651P) so as to disrupt its structure (39), replication at *ori2* is no longer controlled by *crtS* (Figure 4A, B). Because of its limited impact on *ori2* initiation negative regulation, we could transpose the $RctB_{L651P}$ mutation in *V. cholerae*. Even though the L651P mutation increases the level of RctB expression by 20-fold that of WT (Supplementary Figure S10), the number of Chr2 copies is only doubled (Figure 4B) suggesting that RctB concentration level is not a major limiting factor of Chr2 replication control since its overexpression does not considerably increase Chr2 copy number. It was shown in *E. coli* that an increase of RctB concentration does not prevent *crtS* enhancing activity on pORI2 copy number (20,23), thus an increase of RctB concentration induced by the L651P mutation does not explain the loss of *crtS* control on *ori2*.

We analysed the binding affinities of the RctB domain IV mutants to 39m and iterons by monitoring their abilities to repress the PrctB and PrctA promoters respectively (Supplementary Figure S1). All domain IV mutants that are no longer regulated by *crtS* (Figures 3C, 4A, B) also fail to repress the PrctB promoter (Figures 3D, 4C) while retaining their PrctA repression activity (Figure 4C, Supplementary Figure S7). This indicates that binding to 39m, but not to iterons, is impaired in *crtS*-independent mutants. We show *in vitro* that RctBΔIV, RctBΔ157 and RctBΔ147 still bind to iteron, 39m and *crtS*, but no longer oligomerize (Figure 5A, Supplementary Figure S12). Thus, it appears that, *in vivo*, binding to 39m or repression of PrctB depends on RctB cooperative binding capacity. It is known that some transcriptional regulators repress gene expression by forming a nucleoprotein filament on their promoter (40). If this was the case for RctB, we would expect PrctA to be repressed as well, but this is not the case, suggesting that only 39m binding is impaired in *crtS* independent mutants. We have previously reported that oligomerization of RctB on DNA, requires protein-protein interactions mediated by its domain IV (10). Here, we show that all *crtS*-independent RctB mutants exhibit a defect in RctB-RctB self-interaction by domain IV (Figure 5B). More specifically, we found that $RctB_{L651P}$, a *crtS*-independent mutant obtained from a single AA substitution in the extreme C-terminal tail of RctB, is defective for RctB-RctB interactions and PrctB repression. This suggests that these RctB-RctB interactions are involved in the repressing activity of RctB on 29m. However, $RctB_{L651P}$ is weakly involved in the negative regulation of Chr2 copy number, suggesting that these interactions are not involved in *ori2* handcuffing by the 39m.

We can highlight a similarity with the DnaA initiator for which its oligomerization activity is also essential regarding trans-acting sites. In *E.coli,* replication regulation requires a tight control of the cellular concentration of the active initiator DnaA-ATP. Both the reactivation of DnaA–ADP to DnaA–ATP and the hydrolysis of ATP require specific DNA loci (DARS2 and *datA*) and inter-DnaA interactions (41,42). It was shown that mutation in the domain III of DnaA (L290A), which mediates protein self-interaction, severely impairs DARS2-mediated ADP dissociation (41). Thus, it appears that for both chromosome initiators and secondary chromosome initiators (*i.e.* DnaA and RctB),

protein self-interaction is required in the regulation of replication involving a DNA locus other than the origin.

CONCLUDING REMARKS

This study advances our understanding of the coordination of Chr1–Chr2 replication by providing new insights into how Chr2 replication initiation is triggered by *crtS*. Our results indicate that *crtS* acts as an anti-inhibitory site by preventing 39m from negatively regulating *ori2* replication. Thus, we believe that Chr2 replication must be inhibited by RctB binding to 39m for much of the cell cycle (Figure 6A, OFF) and is briefly released when the replication fork passes through the *crtS* site (Figure 6A, ON). The replication of *crtS* would lift the inhibition of Chr2 initiation by the 39m sites, thereby triggering Chr2 replication. Hence, RctB binding to *crtS* may vary depending on its replicative state. Based on past and present results, it is likely that doubling of *crtS* may shift RctB binding from 39m sites to *crtS* allowing *ori2* to be released for replication. We cannot rule out that RctB bound to *crtS* interacts directly with 39m, thereby preventing *ori2* handcuffing, nor can we rule out that a modification of RctB upon binding to *crtS* decreases the affinity of RctB for 39m (10,18,20,23). To verify this, a study of the dynamics of RctB binding at the whole genome level throughout the cell cycle is required.

We also showed that the extreme C-terminal tail of RctB, containing a predicted α-helix, is crucial for the coordination of replication of both chromosomes by *crtS*. Both the C-terminal end of RctB and the activation of *ori2* by *crtS* are found in other *Vibrionaceae* (Supplementary Figure S11; (16)), hence this mechanism is likely to be found in all *Vibrionaceae* species. RctB C-terminal domain has no homologue in other plasmid initiators. The acquisition of an additional domain, here, especially dedicated to *Vibrio* Chr2 replication regulation, illustrates that the development of new functionalities by domain acquisition could be a more general feature of evolution of replication initiators and other bacterial proteins involved in DNA metabolism (Figure 6B). Recently, a unique third domain was identified in TrfA, the Rep initiator of the broad host range RK2 iteron-plasmids. The third domain of TrfA is essential for replication and has led to the definition of a new class of TrfA-like initiators containing three DNA-interacting domains, WH1, WH2 and DBD (43). A similar phenomenon was also observed for integron integrases, where the acquisition of a protein domain led to a functional innovation (44).

SUPPLEMENTARY DATA

Supplementary Data are available at NAR Online.

ACKNOWLEDGEMENTS

We thank Dr Alfonso Soler-Bistué for his help in the development of the Luciferase reporter and sharing of the pASB12 plasmid expressing Renilla Luciferase; Pr. Dhruba Chattoraj for sharing the pTVC11 plasmid; Dr Zeynep Baharoglu, Evelyne Krin and Manon Lang for technical advice on luciferase experiments; Pr. Melanie Blokesch for help with RNA preparation in *Vibrio* and RT-qPCR; Dr Gouzel Karimova, Pr. Daniel Ladant for sharing pKT25 and pUT18C plasmids; Dr Rocio Lopez-Igual for technical advice on bacterial two-hybrid experiments; Dr Sean Kennedy for help with writing the manuscript, and Stilla Technologies for help with the design of RT-dPCR experiments. Molecular graphics and analyses performed with UCSF ChimeraX, developed by the Resource for Biocomputing, Visualization and Informatics at the University of California, San Francisco, with support from National Institutes of Health R01-GM129325 and the Office of Cyber Infrastructure and Computational Biology, National Institute of Allergy and Infectious Diseases. We also would like to thank all our team members for helpful discussions.

FUNDING

Institut Pasteur; Institut National de la Santé et de la Recherche Médicale (INSERM); Centre National de la Recherche Scientifique [CNRS-UMR 3525]; French National Research Agency, Jeunes Chercheurs [ANR-19-CE12-0001]; Laboratoires d'Excellence [ANR-10-LABX-62-IBEID]; F.F. was supported by ANR-10-LABX-62-IBEID and ANR-19-CE12-0001; T.N. was supported by the Ministère de l'Enseignement Supérieur et de la Recherche; J.C. was supported by Institut Pasteur (Cantarini foundation) [ANR-19-CE12-0001, ANR-10-LABX-62-IBEID]. Funding for open access charge: French National Research Agency [ANR-19-CE12-0001].
Conflict of interest statement. None declared.

REFERENCES

1. diCenzo,G.C. and Finan,T.M. (2017) The divided bacterial genome: structure, function, and evolution. *Microbiol. Mol. Biol. Rev.*, **81**, e00019-17.
2. Harrison,P.W., Lower,R.P., Kim,N.K. and Young,J.P. (2010) Introducing the bacterial 'chromid': not a chromosome, not a plasmid. *Trends Microbiol.*, **18**, 141–148.
3. Touchon,M. and Rocha,E.P. (2016) Coevolution of the organization and structure of prokaryotic genomes. *Cold Spring Harb. Perspect. Biol.*, **8**, a018168.
4. Demarre,G. and Chattoraj,D.K. (2010) DNA adenine methylation is required to replicate both *Vibrio cholerae* chromosomes once per cell cycle. *PLos Genet.*, **6**, e1000939.
5. Duigou,S., Knudsen,K.G., Skovgaard,O., Egan,E.S., Lobner-Olesen,A. and Waldor,M.K. (2006) Independent control of replication initiation of the two Vibrio cholerae chromosomes by DnaA and RctB. *J. Bacteriol.*, **188**, 6419–6424.
6. Egan,E.S. and Waldor,M.K. (2003) Distinct replication requirements for the two Vibrio cholerae chromosomes. *Cell*, **114**, 521–530.
7. Chatterjee,S., Jha,J.K., Ciaccia,P., Venkova,T. and Chattoraj,D.K. (2020) Interactions of replication initiator RctB with single- and double-stranded DNA in origin opening of Vibrio cholerae chromosome 2. *Nucleic Acids Res.*, **48**, 11016–11029.
8. Konieczny,I., Bury,K., Wawrzycka,A. and Wegrzyn,K. (2014) Iteron Plasmids. *Microbiol. Spectr.*, **2**, https://doi.org/10.1128/microbiolspec.PLAS-0026-2014.
9. Orlova,N., Gerding,M., Ivashkiv,O., Olinares,P.D.B., Chait,B.T., Waldor,M.K. and Jeruzalmi,D. (2017) The replication initiator of the cholera pathogen's second chromosome shows structural similarity to plasmid initiators. *Nucleic Acids Res.*, **45**, 3724–3737.
10. de Lemos Martins,F., Fournes,F., Mazzuoli,M.V., Mazel,D. and Val,M.E. (2018) Vibrio cholerae chromosome 2 copy number is controlled by the methylation-independent binding of its monomeric initiator to the chromosome 1 *crtS* site. *Nucleic Acids Res.*, **46**, 10145–10156.

11. Jha,J.K., Demarre,G., Venkova-Canova,T. and Chattoraj,D.K. (2012) Replication regulation of *Vibrio cholerae* chromosome II involves initiator binding to the origin both as monomer and as dimer. *Nucleic Acids Res.*, **40**, 6026–6038.
12. Jha,J.K., Li,M., Ghirlando,R., Miller Jenkins,L.M., Wlodawer,A. and Chattoraj,D. (2017) The DnaK chaperone uses different mechanisms to promote and inhibit replication of *Vibrio cholerae* chromosome 2. *MBio*, **8**, e00427-17.
13. Venkova-Canova,T. and Chattoraj,D.K. (2011) Transition from a plasmid to a chromosomal mode of replication entails additional regulators. *Proc. Natl. Acad. Sci. U.S.A.*, **108**, 6199–6204.
14. Ramachandran,R., Jha,J., Paulsson,J. and Chattoraj,D. (2017) Random versus cell cycle-regulated replication initiation in bacteria: insights from studying *Vibrio cholerae* chromosome 2. *Microbiol. Mol. Biol. Rev.*, **81**, e00033-16.
15. Fournes,F., Val,M.E., Skovgaard,O. and Mazel,D. (2018) Replicate Once Per Cell Cycle: Replication Control of Secondary Chromosomes. *Front Microbiol*, **9**, 1833.
16. Kemter,F.S., Messerschmidt,S.J., Schallopp,N., Sobetzko,P., Lang,E., Bunk,B., Sproer,C., Teschler,J.K., Yildiz,F.H., Overmann,J. *et al.* (2018) Synchronous termination of replication of the two chromosomes is an evolutionary selected feature in Vibrionaceae. *PLos Genet.*, **14**, e1007251.
17. Rasmussen,T., Jensen,R.B. and Skovgaard,O. (2007) The two chromosomes of *Vibrio cholerae* are initiated at different time points in the cell cycle. *EMBO J.*, **26**, 3124–3131.
18. Val,M.E., Marbouty,M., de Lemos Martins,F., Kennedy,S.P., Kemble,H., Bland,M.J., Possoz,C., Koszul,R., Skovgaard,O. and Mazel,D. (2016) A checkpoint control orchestrates the replication of the two chromosomes of *Vibrio cholerae*. *Sci. Adv.*, **2**, e1501914.
19. Venkova-Canova,T., Saha,A. and Chattoraj,D.K. (2012) A 29-mer site regulates transcription of the initiator gene as well as function of the replication origin of Vibrio cholerae chromosome II. *Plasmid*, **67**, 102–110.
20. Baek,J.H. and Chattoraj,D.K. (2014) Chromosome I controls chromosome II replication in Vibrio cholerae. *PLos Genet.*, **10**, e1004184.
21. Venkova-Canova,T., Srivastava,P. and Chattoraj,D.K. (2006) Transcriptional inactivation of a regulatory site for replication of Vibrio cholerae chromosome II. *Proc. Natl. Acad. Sci. U.S.A.*, **103**, 12051–12056.
22. Jha,J.K., Ghirlando,R. and Chattoraj,D.K. (2014) Initiator protein dimerization plays a key role in replication control of Vibrio cholerae chromosome 2. *Nucleic Acids Res.*, **42**, 10538–10549.
23. Ramachandran,R., Ciaccia,P.N., Filsuf,T.A., Jha,J.K. and Chattoraj,D.K. (2018) Chromosome 1 licenses chromosome 2 replication in Vibrio cholerae by doubling the *crtS* gene dosage. *PLos Genet.*, **14**, e1007426.
24. Karimova,G., Pidoux,J., Ullmann,A. and Ladant,D. (1998) A bacterial two-hybrid system based on a reconstituted signal transduction pathway. *Proc. Natl. Acad. Sci. U.S.A.*, **95**, 5752–5756.
25. Madic,J., Zocevic,A., Senlis,V., Fradet,E., Andre,B., Muller,S., Dangla,R. and Droniou,M.E. (2016) Three-color crystal digital PCR. *Biomol. Detect. Quantif.*, **10**, 34–46.
26. Lo Scrudato,M. and Blokesch,M. (2012) The regulatory network of natural competence and transformation of Vibrio cholerae. *PLoS Genet.*, **8**, e1002778.
27. Soler-Bistue,A., Aguilar-Pierle,S., Garcia-Garcera,M., Val,M.E., Sismeiro,O., Varet,H., Sieira,R., Krin,E., Skovgaard,O., Comerci,D.J. *et al.* (2020) Macromolecular crowding links ribosomal protein gene dosage to growth rate in Vibrio cholerae. *BMC Biol.*, **18**, 43.
28. Pal,D., Venkova-Canova,T., Srivastava,P. and Chattoraj,D.K. (2005) Multipartite regulation of rctB, the replication initiator gene of *Vibrio cholerae* chromosome II. *J. Bacteriol.*, **187**, 7167–7175.
29. Jumper,J., Evans,R., Pritzel,A., Green,T., Figurnov,M., Ronneberger,O., Tunyasuvunakool,K., Bates,R., Zidek,A., Potapenko,A. *et al.* (2021) Highly accurate protein structure prediction with AlphaFold. *Nature*, **596**, 583–589.
30. Mirdita,M., Ovchinnikov,S. and Steinegger,M. (2021) ColabFold - making protein folding accessible to all. bioRxiv doi: https://doi.org/10.1101/2021.08.15.456425, 15 August 2021, preprint: not peer reviewed.
31. Pettersen,E.F., Goddard,T.D., Huang,C.C., Meng,E.C., Couch,G.S., Croll,T.I., Morris,J.H. and Ferrin,T.E. (2021) UCSF ChimeraX: structure visualization for researchers, educators, and developers. *Protein Sci.*, **30**, 70–82.
32. Alias,M., Ayuso-Tejedor,S., Fernandez-Recio,J., Cativiela,C. and Sancho,J. (2010) Helix propensities of conformationally restricted amino acids. Non-natural substitutes for helix breaking proline and helix forming alanine. *Org. Biomol. Chem.*, **8**, 788–792.
33. Srivastava,P. and Chattoraj,D.K. (2007) Selective chromosome amplification in Vibrio cholerae. *Mol. Microbiol.*, **66**, 1016–1028.
34. Ciaccia,P.N., Ramachandran,R. and Chattoraj,D.K. (2018) A requirement for global transcription factor Lrp in licensing replication of *Vibrio cholerae* chromosome 2. *Front Microbiol*, **9**, 2103.
35. Wegrzyn,K.E., Gross,M., Uciechowska,U. and Konieczny,I. (2016) Replisome assembly at bacterial chromosomes and iteron plasmids. *Front Mol Biosci*, **3**, 39.
36. Ozaki,S., Kawakami,H., Nakamura,K., Fujikawa,N., Kagawa,W., Park,S.Y., Yokoyama,S., Kurumizaka,H. and Katayama,T. (2008) A common mechanism for the ATP-DnaA-dependent formation of open complexes at the replication origin. *J. Biol. Chem.*, **283**, 8351–8362.
37. Kawasaki,Y., Matsunaga,F., Kano,Y., Yura,T. and Wada,C. (1996) The localized melting of mini-F origin by the combined action of the mini-F initiator protein (RepE) and HU and DnaA of Escherichia coli. *Mol. Gen. Genet.*, **253**, 42–49.
38. Kelley,W.L. and Bastia,D. (1992) Activation in vivo of the minimal replication origin beta of plasmid R6K requires a small target sequence essential for DNA looping. *New Biol.*, **4**, 569–580.
39. Lefevre,F., Remy,M.H. and Masson,J.M. (1997) Alanine-stretch scanning mutagenesis: a simple and efficient method to probe protein structure and function. *Nucleic. Acids. Res.*, **25**, 447–448.
40. Lim,C.J., Lee,S.Y., Kenney,L.J. and Yan,J. (2012) Nucleoprotein filament formation is the structural basis for bacterial protein H-NS gene silencing. *Sci. Rep.*, **2**, 509.
41. Kasho,K., Fujimitsu,K., Matoba,T., Oshima,T. and Katayama,T. (2014) Timely binding of IHF and Fis to DARS2 regulates ATP-DnaA production and replication initiation. *Nucleic Acids. Res.*, **42**, 13134–13149.
42. Kasho,K. and Katayama,T. (2013) DnaA binding locus datA promotes DnaA-ATP hydrolysis to enable cell cycle-coordinated replication initiation. *Proc. Natl. Acad. Sci. U.S.A.*, **110**, 936–941.
43. Wegrzyn,K., Zabrocka,E., Bury,K., Tomiczek,B., Wieczor,M., Czub,J., Uciechowska,U., Moreno-Del Alamo,M., Walkow,U., Grochowina,I. *et al.* (2021) Defining a novel domain that provides an essential contribution to site-specific interaction of Rep protein with DNA. *Nucleic Acids Res.*, **49**, 3394–3408.
44. Escudero,J.A., Nivina,A., Kemble,H.E., Loot,C., Tenaillon,O. and Mazel,D. (2020) Primary and promiscuous functions coexist during evolutionary innovation through whole protein domain acquisitions. *Elife*, **9**, e58061.